Reactive and Functional Polymers 193 (2023) 105764

Contents lists available at ScienceDirect

Reactive and Functional Polymers

journal homepage: www.elsevier.com/locate/react

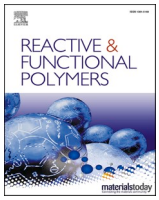

Towards fast relaxation rates and creep resistance in disulfide vitrimer-like materials

Adrià Roig [a], Valeria D'Agostino [b], Àngels Serra [a,*], Silvia De la Flor [b,*]

[a] Universitat Rovira i Virgili, Department of Analytical and Organic Chemistry, C/ Marcel·lí Domingo 1, Edif. N4, Tarragona 43007, Spain
[b] Universitat Rovira i Virgili, Department of Mechanical Engineering, Av. Països Catalans 26, Tarragona 43007, Spain

ARTICLE INFO

Keywords:
Vitrimer
Disulfide
Fast relaxation
Creep resistance
Self-healing
Self-welding

ABSTRACT

Reaching a delicate balance between polymer flow for reprocessing and mechanical robustness at service temperatures remains a challenge in designing dynamic polymer networks. The demand for creep-resistant materials with fast relaxation rates at relatively low temperatures is a crucial research topic in the academic world. In this study, we present the preparation of a series of disulfide vitrimeric materials by curing two commercially available aromatic and aliphatic epoxy resins and cystamine. Through careful variation of the proportions between the epoxy resins, the properties of the final materials can be properly tailored. The completion of the curing was confirmed using FTIR spectrometry, and the thermal stability of all materials was evaluated by TGA. The thermomechanical properties were investigated using DMA analysis, obtaining glass transition temperatures (T_gs) above 60 °C and high rigidity in the glassy state depending on the proportion of the aromatic resin.

Extensive stress relaxation tests unveiled remarkable vitrimeric behavior, with all materials capable of relaxing 63% of the initial stress in less than 2 min at 140 °C. The in-depth creep experiments not only allowed for determining material viscosity at high temperatures and the topology freezing temperatures (T_vs) but also offered control over dynamic stability at room temperature, depending on the initial formulation composition. Dilatometry and tensile tests provided further insights into the materials' characteristics.

The self-healing and self-welding behavior enabled by the disulfide metathesis exchange reactions were also evaluated, revealing a total self-healing recovery process with short times and comparable tensile modulus in the welded samples. The facile preparation, commercial availability of monomers, and excellent thermosetting and vitrimeric properties highlight the immense potential of this series of materials.

1. Introduction

Nowadays, covalent adaptable networks (CANs) are gaining interest thanks to their ability to combine the excellent mechanical performance of thermosets and the recycling, reprocessing, and reshaping ability of thermoplastics [1]. These materials include dynamic bonds in their structure that, through reversible chemical processes triggered by external stimulus, usually temperature, allow the network rearrangement [2]. This means that CANs can behave as thermosets at room temperature. However, when a certain temperature is exceeded, reversible reactions take place, altering their behavior from a viscoelastic solid to a fluid-like plastic. Depending on the mechanism of these exchangeable chemical processes, CANs can be classified into two main groups. The first class, the dissociative, is characterized by a two-step mechanism in which, first, a bond is broken and then re-formed in another place. This induces the loss of the network integrity and, thus, a sudden drop in the viscosity that sometimes makes them difficult to be processed. On the other hand, the associative CANs or vitrimers undergo concertedly without losing their network integrity and always keeping the crosslinking density constant. In vitrimers, a relationship between viscosity and temperature is established following an Arrhenius dependence like silica [3]. Many studies have been performed regarding all types of CANs since Prof. Leibler described them in 2011, encompassing several chemical reactions [3–11]. Recently Dichtel et al. reported the preparation of a new type of CANs: vitrimer-like polymers [12]. Chemically, the mechanism of the exchange reactions of these materials works through a dissociative pathway, but physically, there is not a sudden drop in viscosity like dissociative CANs. However, there is a gradual decrease in the viscosity with the temperature as vitrimers. This particularity makes them very interesting for industrial applications like

* Corresponding authors.
E-mail address: angels.serra@urv.cat (À. Serra).

https://doi.org/10.1016/j.reactfunctpolym.2023.105764
Received 24 July 2023; Received in revised form 25 October 2023; Accepted 26 October 2023
Available online 29 October 2023

self-healing, reshaping or self-welding. For this reason, many researchers are focusing their attention on the preparation of vitrimer-like materials [13–16]. Among all chemical reactions present in CANs that can undergo a chemical dissociative mechanism but, at the same time, follow an Arrhenius-type dependence of the viscosity with temperature, the disulfide metathesis is the most well-studied. Rekondo and co-workers reported the preparation of aromatic disulfide epoxy vitrimers by the curing of diglycidyl ether of bisphenol A (DGEBA) with *ortho* and *para* diamino disulfide in stoichiometric and in off-stoichiometric conditions with an excess of free amines, and with a catalyst [17]. They stated that the presence of free amines or catalysts in the materials enhanced the stress relaxation rates allowing tailoring of the dynamic and mechanical properties of the final materials. Moreover, they reported that the vitrimer-like properties of some of these materials revealed the drop of the modulus at low frequencies. Yamawake et al. explored the role of internal tertiary amines in disulfide covalent adaptable networks [18]. They prepared two different materials with the same segmental mobility and cross-linking density, one with covalently linked tertiary amines and one without amines, for a better comparison. They demonstrated the the stress relaxation rates and creep resistance enhancement with the sample containing tertiary amines. Moreover, through electron spin resonance (ESR), they revealed the formation of thiyl radicals during the bond exchange, thus demonstrating the dissociative pathway of the mechanism, even maintaining a gradual decrease of the viscosity with the temperature. As far as we know, the formation of thiyl radicals in aliphatic disulfide moieties it is not reported and, therefore, the dissociative mechanism is still not verified for this type of structures.

In this context, Li et al. explored the dynamicity of aliphatic disulfide materials in the field of adhesion [19]. By preparing materials using cystamine as a crosslinker, they discovered their capability to fill voids in the adhesion plates and improve the surface wettability. By performing an annealing of the polymer, they increase the lap shear strength by a factor of 4 in comparison to the one that was not annealed and by a factor of 2 when compared to annealed thermoset material indicating the enhanced performance of these aliphatic disulfide moieties. Guerre and co-workers also used cystamine to prepare cross-linked materials with an epoxy-derivative of vanillin [20]. They compared the dynamicity of aromatic disulfide bonds with aliphatic disulfide bonds by combining both aromatic and aliphatic disulfides in the same materials. They reported that with only 20% of cystamine and 80% of 4AFD they could achieve similar relaxation rates compared to pure cystamine materials demonstrating the enhancement in the exchange reactions when aliphatic disulfide bonds are present in the network even maintaining high values of glass transition temperatures. More recently, in our group, we reported the preparation of bio-based epoxy vitrimers by using an epoxy derivative of eugenol and a combination of cystamine and tris-(2-aminoethyl) amine (TREN) [21]. All materials displayed high values of T_g (above 60 °C) and fast relaxation rates. More interesting, a compromise between the content of aliphatic tertiary amines and the concentration of disulfide bonds was found, obtaining faster relaxation times when the material was prepared with 25% of TREN and 75% of cystamine instead of with only cystamine thus indicating a possible catalytic effect of internal covalent tertiary amines on the disulfide exchange.

Balancing material flow for thermal reprocessability with dimensional stability during service use still remains a key design challenge in the field of dynamic covalent polymer networks. The use of latent catalysts, protecting groups and phase separation, the incorporation of substituents that either enhance or inhibit the activation rate, or the use of dynamic covalent bonds with high reaction enthalpy are employed to prepare dynamic networks while avoiding creep at services temperatures [22]. Even the incorporation of permanent bonds (maximum of 40%) in the polymer structure may still provide good dynamicity to the network while controlling the flow at temperatures of use, as demonstrated by Torkelson and co-workers [23]. Nevertheless, this investigation field is in its early stages, and some efforts still need to be done.

Taking all this into account, this study presents a series of vitrimeric materials obtained by an epoxy-amine condensation from commercially available monomers such as triglycidyl-*p*-aminophenol (TGAP) and 1,6-hexanediol diglycidyl ether (HDGE) as epoxy precursors and cystamine (Cys) as the amine cross-linker (Fig. 1). The presence of disulfide linkages as dynamic bonds in the structure of Cys enables the vitrimeric behavior.

The thermomechanical properties of the materials can be tailored by varying the proportions of both epoxy monomers. As the stress relaxation tests demonstrated, the materials exhibit high T_gs above 50 °C and very fast relaxation rates at high temperatures.. A complete creep analysis was also performed to determine the materials' topology freezing temperature (T_v), their relationship with temperature below and above T_g, and the creep behavior at service temperatures. By increasing the proportion of the aromatic epoxy resin, creep at room temperature is expected to be minimized while preserving short relaxation times [23,24]. Stress-strain tests were also performed to study the mechanical behavior, revealing good mechanical performance in the tested materials. The prepared materials also showed outstanding self-healing and self-welding properties, highlighting their potential use in the industrial field.

2. Experimental section

2.1. Materials

Cystamine dihydrochloride (97%, Cys, 38.07 g /eq.) and triglycidyl-*p*-aminophenol (99%, TGAP, 92.44 g/eq.) were purchased from Sigma Aldrich. 1,6-Hexanediol diglycidyl ether (HDGE, 115.15 g/eq.) was kindly supplied from Epotec. Potassium hydroxide (KOH) and anhydrous magnesium sulfate ($MgSO_4$) were purchased from Scharlau.

2.2. Preparation of cystamine (Cys)

To prepare cystamine, 8 g of cystamine dihydrochloride and 6 g of KOH were dissolved in 100 mL of distilled water and stirred at room temperature for 30 min. The resulting mixture was extracted four times with 100 mL of dichloromethane (DCM). The organic layers were combined, dried over anhydrous $MgSO_4$, and filtered, and the solvent was removed in a rotary evaporator, obtaining 3.9 g of a yellowish viscous oil (Cys). The pure cystamine must be used immediately after being obtained or it must be kept in a fridge.

^{1}H NMR ($CDCl_3$; δ, ppm): 2.95 (t, 4H); 2.70 (t, 4H); 1.28 (s, 4H) (see Fig. S1).

^{13}C NMR ($CDCl_3$; δ, ppm): 42.55, 40.60 (see Fig. S2).

2.3. Preparation of epoxy vitrimer-like materials

All materials were prepared by mixing TGAP and HDGE with the corresponding amount of Cys in molar stoichiometric conditions NH/epoxy 1:1 in a vial and vigorously stirred. Then, the formulation was poured into a Teflon mold with dimensions of 30 × 5 × 1.5 mm^3 and cured for 3 h at 100 °C and post-cured for 1 h at 140 °C and 2 h at 160 °C. Samples with different amounts of epoxy resins were prepared and encoded as PolyX%, where X represents the percentage of NH groups of Cys reacting with epoxy groups of TGAP. As a consequence, the missing percentage refers to the NH groups of Cys reacting with epoxy groups provided by the other epoxy resin, HDGE. The composition of the different materials is depicted in Table 1.

2.4. Characterization techniques

A Jasco FTIR-680 Plus spectrometer equipped with an attenuated total reflection accessory (ATR) (Golden Gate, Specac Ltd., Teknokroma)

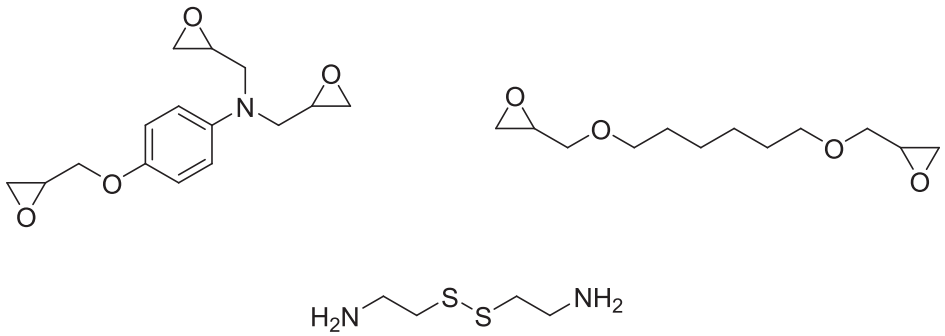

Fig. 1. Chemical structures of triglycidyl-*p*-aminophenol (TGAP) (top left), 1,6-hexanediol diglycidyl ether (HDGE) (top right) and cystamine (Cys) (bottom).

Table 1
Amounts of each component in the initial formulations and concentration of aliphatic amines in the final materials.

Sample	TGAP (meq. epoxide)	TGAP (mg)	HDGE (meq. epoxide)	HDGE (mg)	Cys (meq. NH)	Cys (mg)	[$N_{alifatic}$] mmol/g
Poly50%	5.25	485	5.25	605	10.50	400	7.05
Poly60%	6.30	580	4.20	485	10.50	400	7.17
Poly70%	7.35	680	3.15	365	10.50	400	7.27
Poly80%	8.40	775	2.10	245	10.50	400	7.40

was used to record the FTIR spectra of the mixture before and after the curing procedure. Real-time spectra were recorded in the wavenumber range between 4000 and 600 cm^{-1} with a resolution of 4 cm^{-1} and averaged over 20 scans. The disappearance of the characteristic absorbance peak of the epoxy group at 915 cm^{-1} and the appearance of the peak corresponding to O-H at 3300 cm^{-1} were used to confirm the completion of the epoxy-amine condensation reaction. The thermal stability of the materials was evaluated using a Mettler Toledo TGA 2 thermobalance. Cured samples weighing around 10 mg were degraded between 30 and 600 °C at a heating rate of 10 °C min^{-1} under a N_2 atmosphere with a flow rate of 50 cm^3 min^{-1}. The thermomechanical properties were studied using a DMA Q800 (TA Instruments) equipped with a film tension clamp. Prismatic rectangular samples with dimensions of around 30 × 5 × 1.5 mm^3 were analyzed from 0 to 180 °C at 1 Hz, with 0.1% strain at a heating rate of 2 °C min^{-1}. Tensile stress-relaxation tests were conducted in the same equipment on samples with the same dimensions as previously defined. The samples were firstly equilibrated at the relaxation temperature for 3 min, and a constant strain of 1% was applied, measuring the consequent stress level as a function of time. Then, the strain was removed, and the process was repeated every 5 °C until the final test temperature was reached. The relaxation-stress $\sigma(t)$ was normalized by the initial stress σ_0, and the relaxation times (τ) were determined as the time necessary to relax to $0.37\sigma_0$, i.e. ($\sigma = 1/e\sigma_0$). With the relaxation times obtained at each temperature, the activation energy values (E_a) were calculated using an Arrhenius-type equation:

$$ln(\tau) = \frac{E_a}{RT} - lnA \quad (1)$$

where τ is the time needed to attain a given stress-relaxation value ($0.37\sigma_0$), A is the pre-exponential factor, and R is the gas constant.

To determine the viscosity at each temperature, a series of creep experiments were carried out with the same DMA Q800 instrument equipped with the film tension clamp at temperatures between 0 and 180 °C, increasing 10 °C in each scan. To perform the tests, the samples were equilibrated for 3 min at the selected temperatures, and a stress level of 0.1 MPa was applied for 30 min. The viscosity η (Pa·s) was obtained from the creep plots: first, the strain rate ($\dot{\varepsilon}$) was determined from the slope of the ε-time curves, and then the viscosity was calculated using the following expression:

$$\eta = \frac{\sigma}{\dot{\varepsilon}} \quad (2)$$

and represented in front of T_g/T, thus obtaining the Angell Fragility plot. In addition, individual creep tests were conducted at 0 °C and 25 °C for each sample to analyze the creep behavior at service temperatures. Samples were equilibrated for 3 min at the selected temperature, and a determined stress was applied for 30 min followed by a recovery time of 30 min. In each case, the stress level was chosen to ensure that the sample remained in the viscoelastic regime. Dilatometry experiments in tension were performed in the same DMA instrument using a film tension clamp on samples with the same dimensions previously described. The sample length was continuously measured while increasing the temperature at a heating rate of 1 °C min^{-1} from −30 to 200 °C. A slight stress of 0.01 MPa was applied during the experiment to avoid buckling. For the self-healing tests, a manual press with a round steel indenter of diameter 2.5 mm was used to make plastic indentations on the sample's surface by applying increasing loads from 31.25 kg (306 MPa) to 150 kg (360 MPa). Subsequently, the samples were heated in an oven at 160 °C for 2 min, exploring from time to time the evolution of the indentation in the healing process by taking pictures with a Digital Microscope Leica DMS1000. To explore the self-welding ability, tensile tests were conducted at room temperature using an electromechanical universal testing machine (Shimadzu AGS-X) with a 1 kN load cell at 5 mm min^{-1}. Dog-bone-shaped samples of virgin and self-welded materials were tested until failure to determine and compare their strength at break and tensile modulus.

3. Results and discussion

3.1. Curing procedure and thermal properties of the materials

All materials were prepared under stoichiometric epoxy/NH conditions and cured according to the previously described procedure to obtain brownish and transparent samples, as can be seen in Fig. 2a. To check the completion of the epoxy-amine condensation reaction, FTIR spectra were recorded on the initial formulations and the materials after the curing and post-curing (Fig. 2b).

As can be seen, the characteristic band at 915 cm^{-1} corresponding to the epoxy groups of the initial resins completely vanished. In contrast, a broad band at 3300 cm^{-1} related to the hydroxyl groups generated by the ring opening of the epoxide with the amines appeared, which

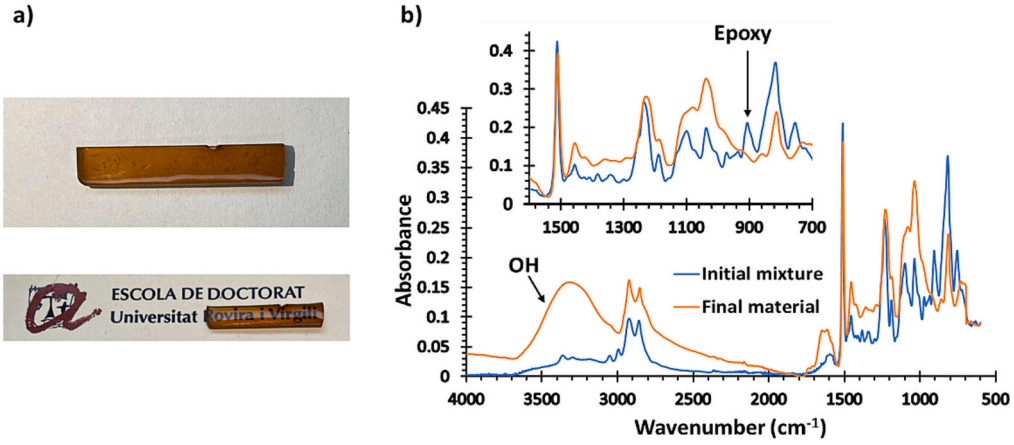

Fig. 2. a) Pictures of the cured poly70% and b) FTIR spectra of the initial formulation and the final material for poly70%.

confirmed the end of the condensation reaction and the proper election of the curing parameters.

The thermal stability of the cured materials was studied by thermogravimetry (TGA). Fig. 3 shows the TGA curves and their derivatives for all samples prepared, and Table 2 collects the most significant data extracted. It can be observed that all materials showed excellent stability until almost 200 °C, which allows a safe relaxation test below that temperature. Moreover, the higher the content of the aromatic epoxy resin in the material, the higher the stability and char residue at 600 °C due to the higher proportion of aromatic rings in the sample. Finally, all materials showed similar DTG curves revealing two maximum degradation rates, a first one at around 260 °C which can be probably ascribed to the degradation of the disulfide bonds, and a second one at almost 330 °C which may correspond to the degradation of the poly(hydroxyamine) network.

3.2. Study of the thermomechanical properties

The thermomechanical behavior of all materials prepared was investigated by DMA analysis. Fig. 4 presents the evolution of the tan δ curves and the storage modulus with temperature, and the most relevant data obtained from these results are presented in Table 2.

As it can be seen from the data, all samples showed good homogeneity (see FWHM at Table 2) and the T_gs, determined from the maximum of the peaks of the *tan* δ curves, are far above room temperature, being 62 °C for poly50% and 112 °C for poly80%. The higher content of aromatic epoxy resin in the formulation, the higher the T_g of the samples due to the rigidity and the higher cross-linking density in the final material. The same trend can be detected in the storage modulus, where poly80% is the most rigid sample in the glassy state, and poly50% is the softer. The storage modulus in the rubbery state also displayed higher values when the proportion of TGAP in the sample was higher due to its tri-functionality that provides a higher cross-linking density in the material. In any case, all materials revealed high values of $E'_{rubbery}$, leading to considerable compact networks. To evaluate the vitrimeric-like behavior of the materials prepared, stress relaxation tests were performed by DMA, which allowed the determination of the time and temperature-dependence relaxation of all the materials. These results can be observed in Fig. 5, and the characteristic data extracted from the relaxation curves are presented in Table 3.

The stress relaxation curves reveal that all the materials can relax extremely fast the 63% of the initial stress ($\sigma = 0.37\sigma_0$) in less than 0.40 min for poly50%, 0.45 min for poly60%, 1.10 min for poly70%, and 1.50 min for poly80% without the need of an external catalyst increasing the relaxation time with the amount of TGAP in the material. It is reported in the literature that the tertiary amines generated after the epoxy-amine condensation can catalyze the disulfide metathesis by the nucleophilic attack of these amines to the S-S bond, generating a thiolate which can attack another disulfide bond [18]. Despite that on increasing the content of aromatic epoxy resin in the material, the proportion of aliphatic nucleophilic tertiary amines increases (Table 1), the higher rigidity provided from the aromatic ring and the higher functionality results in an increase of the relaxation time. Consequently, as can be observed, when the content of the aromatic epoxy resin increases in the

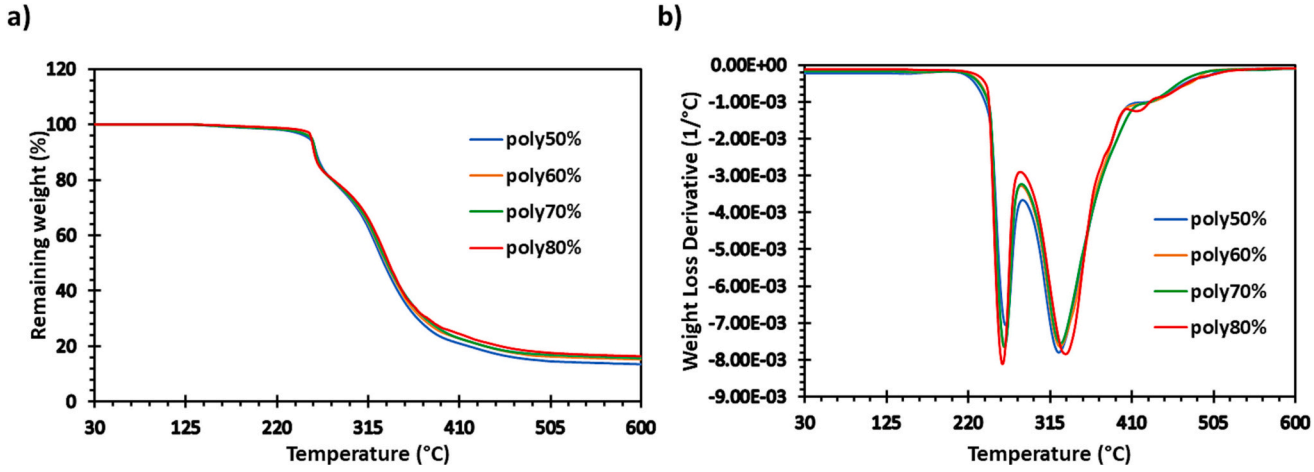

Fig. 3. a) Thermogravimetric curves and b) DTG curves of all materials prepared.

Table 2
Thermogravimetric and thermomechanical data of all the materials obtained. Coefficients of variation less than 2% for $T_{tan\ \delta}$ and FWHM and less than 5% for storage moduli (E').

Sample	$T_{1\%}$ [a] (°C)	$T_{2\%}$ [b] (°C)	T_{max} [c] (°C)	Char Yield [d] (%)	E'_{glassy} [e] (MPa)	$E'_{rubbery}$ [f] (MPa)	$T_{tan\ \delta}$ [g] (°C)	FWHM [h]
Poly50%	198.1	215.2	263.3/325.0	13.5	2450	16.7	62	23.0
Poly60%	200.4	215.9	261.5/326.3	15.2	2775	25.0	74	24.3
Poly70%	201.9	216.7	261.8/327.6	15.8	2836	36.9	96	25.3
Poly80%	208.6	225.3	259.8/333.2	16.4	3220	52.1	112	29.6

[a] Temperature of 1% of weight loss.
[b] Temperature of 2% of weight loss.
[c] Temperature of the maximum rate of degradation.
[d] Char residue at 600 °C.
[e] Storage modulus in the glassy state at T_g – 50 °C.
[f] Storage modulus in the rubbery state at T_g + 50 °C.
[g] Temperature at the maximum of tan δ peak at 1 Hz.
[h] Full width at half maximum of tan δ peak.

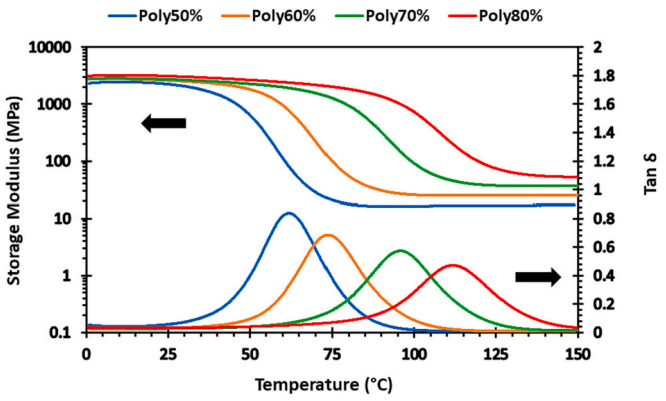

Fig. 4. Evolution of the storage modulus and *tan* δ with temperature for all materials prepared.

sample, the materials relax the stress more slowly. Another factor that can reduce the rate of relaxation is the rigidity of TGAP in comparison to that of HDGE. This fact, together with the higher functionality of TGAP, leads to a more rigid and closed network with higher topological constraints for structural changes. It is worth mentioning that a slight plastic deformation effect is produced in all the materials when continuous stress relaxation tests are performed. This produces a slight decrease in the maximum relaxation value reached.

Vitrimeric materials are widely known to display a temperature dependence that follows an Arrhenius-type relationship [12,25]. This dependence occurs when the chemical exchange reactions control the viscosity. Consequently, the temperature-viscosity relationship is similar to inorganic silica materials. To further investigate the vitrimeric behavior, the relaxation curves were used to determine the time needed for the initial stress to decrease to e^{-1} ($\sigma/\sigma_0 = 0.37$) at different temperatures. By fitting the data to an Arrhenius-type equation, the activation energy (E_a) of the topological rearrangement for all materials can be calculated (see Fig. 6 and Table 3).

The Arrhenius plots revealed that the higher the content of TGAP in the material, the higher dependence of the relaxation time with the temperature, being the poly80% the material with the highest E_a (64 kJ/mol) and the poly50% the lowest (22 kJ/mol). This is directly linked with the hypothesis previously mentioned that even the poly80% is the material that contains more aliphatic tertiary amines (see Table 1) capable to catalyze the exchange reaction, the high rigidity and cross-linking density hinders the disulfide metathesis and therefore, a higher activation energy is required to allow the exchange mechanism [18,21]. It is worthy to mention that E_a values of poly80% and poly70%, and poly60% and poly50% are similar, but the differences in the pre-exponential factor (ln*A*) allow faster relaxation times at a determined temperature when the content of TGAP is lower. Moreover, even the disulfide exchange is able to undergo via a dissociative-radical mechanism, all materials fitted properly the Arrhenius plot, confirming a vitrimeric-like behavior.

3.3. Study of the viscosity and creep behavior

To make a deeper study of the effect of temperature on the viscoelastic behavior of these materials, creep tests from 30 °C to 140 °C were performed by DMA (see Figs. S3-S6). It can be observed that when a constant stress is applied at different temperatures, the strain increases with time with a different rate depending on the temperature, being negligible under the T_g and remarkable above it. According to that, these materials behave like a viscoelastic vitrimer and not as a conventional rubber thermoset which would show a slight increase in the strain rate under a constant stress. From these results, the viscosity at each temperature can be calculated as the inverse of the slope of the strain evolution over time (strain rate, $\dot{\varepsilon}$). Fig. 7a shows the plot of the viscosity at each temperature for all the materials.

It can be seen that materials with a higher content of the aromatic epoxy resin present a steeper viscosity decrease until their glass transition temperature being fairly constant after this temperature. Nevertheless, in the case of poly50% and poly60%, the viscosity decreases in the whole interval of temperatures, even above their T_gs. The first drop of the viscosity can be attributed to the glassy to rubber transition of the polymers. When this transition is overpassed, a higher decrease of the viscosity can be observed in the materials with less amount of TGAP due to its higher mobility and flexibility that make the exchange processes more likely to occur (dynamic transition). These phenomena are overlapped but they can be more appreciated beyond the T_g in materials with less content of aromatic epoxy resin. A critical parameter in the characterization of vitrimeric materials is the topology freezing temperature (T_v). Chemically, this parameter accounts for the temperature below which the exchange between dynamic bonds is negligible. Moreover, this temperature is defined as the one at which the material reaches a viscosity of 10^{12} Pa·s [3]. From Fig. 7a, the T_v of all the materials can be obtained by assuming $\log(\eta_{Tv}) = 12$ (see Table 3). It can be appreciated that, as expected, the T_vs increase when a higher proportion of TGAP is present in the sample. The higher the functionality and the higher content of aromatic rings, the lower the mobility and flexibility of the chains, which leads to a lower probability of the exchange reactions taking place. As seen, the T_v in all cases was below the T_g of the corresponding materials.

The Angell fragility plot is represented in Fig. 7b, showing that the evolution of the viscosity with relative temperature of all materials differs from a classical vitrimer, laying below the vitreous silica relationship. Above the topology freezing temperature, the exchange reactions become active, and both the relaxation time and viscosity exhibit

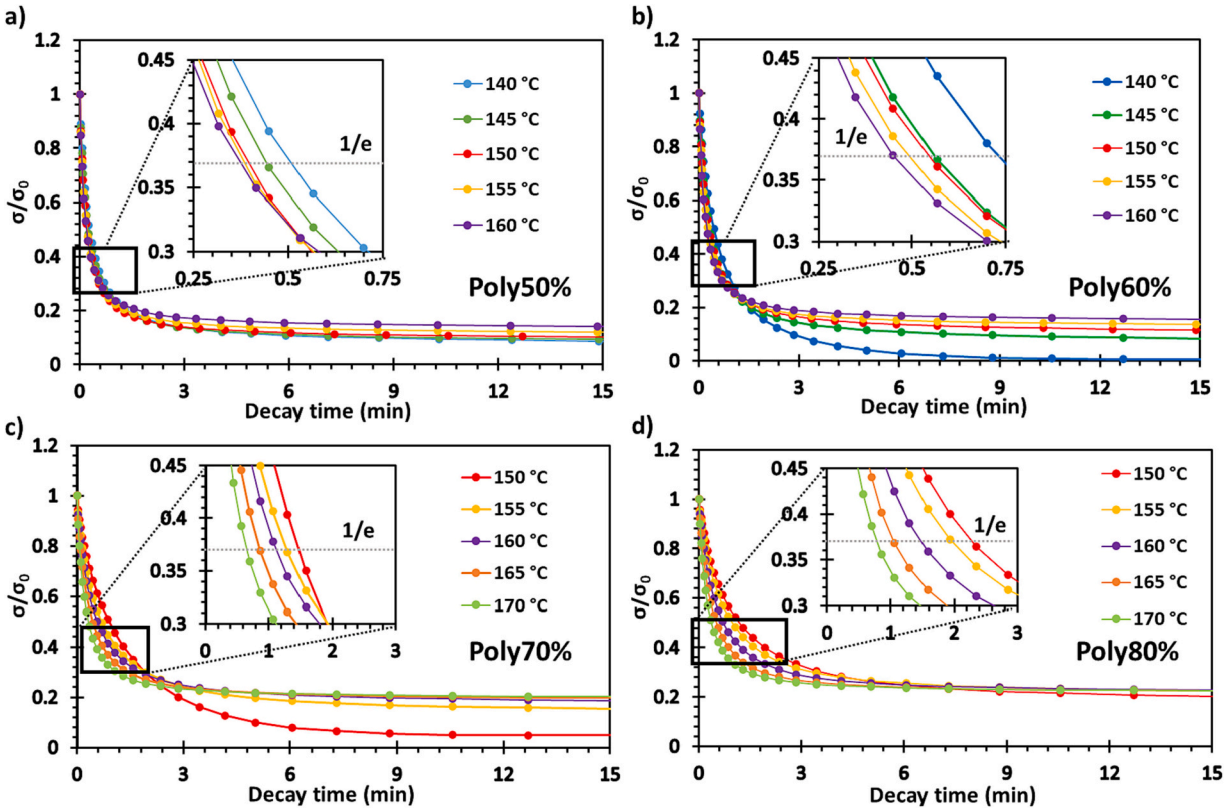

Fig. 5. Normalized stress relaxation plots as a function of time at various temperatures during 15 min for poly50% (a), poly60% (b), poly70% (c), and poly80% (d) samples.

Table 3
Relaxation time, activation energy and adjusting parameters of the Arrhenius equation and activation energy, topology freezing temperature and fragility index of all materials prepared.

Stress relaxation tests					Creep tests		
Sample	$\tau_{0.37}$[a] (min)	ln *A* (min)	r^2	E_a[b] (kJ/mol)	E_a[c] (kJ/mol)	$T_{v(\eta)}$[d] (°C)	n[e]
Poly50%	0.40	3.0	0.9709	22	32	10	32
Poly60%	0.45	4.8	0.9902	35	37	23	37
Poly70%	1.10	11.2	0.9881	54	41	37	41
Poly80%	1.50	13.6	0.9926	64	46	64	46

[a] Time to reach a value of $\sigma/\sigma_0 = 0.37$ at 160 °C.
[b] Activation energy deduced from the Arrhenius plots.
[c] Activation energy deduced from the Angell Fragility plot.
[d] Topology freezing temperature calculated from the creep tests at a viscosity of 10^{12} Pa·s.
[e] Fragility index, in which $n = 16.5$ is the corresponding value for vitreous silica.

behavior consistent with the Arrhenius law, similar to inorganic silica materials, which are considered ideal strong liquids [26,27]. This behavior is in contrast to that observed in thermoplastics and dissociative covalent adaptable networks, which behave as "fragile liquids" because of at high temperatures, the viscosity suffers a sudden drop. For this reason, these materials herein can be categorized as "vitrimer-like" materials. Moreover, from this graph, it is possible to obtain the activation energy for each material from the creep behavior (see Table 3). As can be seen, the activation energies are similar to those obtained from the Arrhenius plot presenting the same trend: the calculated E_as are lowest for samples with lower content of aromatic epoxy resin.

To confirm the observed behavior, the relaxation process was also investigated by dilatometry experiments (Fig. S7). In this case, classical thermosets with a permanently crosslinked network exhibit a slight and constant strain increase with temperature with a small non-linear region corresponding to the glass transition. Conversely, in the case of vitrimers, two different changes in the slope of the strain-temperature curve could be observed: a first one at $T = T_g$ and a second one when the exchange reactions occur ($T = T_v$)[28–30]. In Fig. S7 these two changes are not visible because the relaxation process of the interchange reactions and the mobility of the polymer chains are overlapped, as was previously deduced from the creep tests in which all T_v values were below the corresponding T_gs.

Isothermal creeps at 0 and 25 °C were performed in DMA to determine the effect of temperature on the creep behavior at services temperatures. Fig. 8a shows the creep plots of all the vitrimer-like materials at 0 °C, while Fig. 8b shows the result for the same creep test but at 25 °C. As it can be seen at 0 °C, poly80% and poly70% behave as traditional thermosets without creep and a complete strain recovery. On the other hand, poly60% and poly50% present a slight strain increase with the time and a longer recovery process after the stress is released. This can be ascribed to a more deformable molecular structure which entails a more viscous behavior in comparison to poly80% and poly70%. This can be clearly seen in the loss modulus evolution with temperature

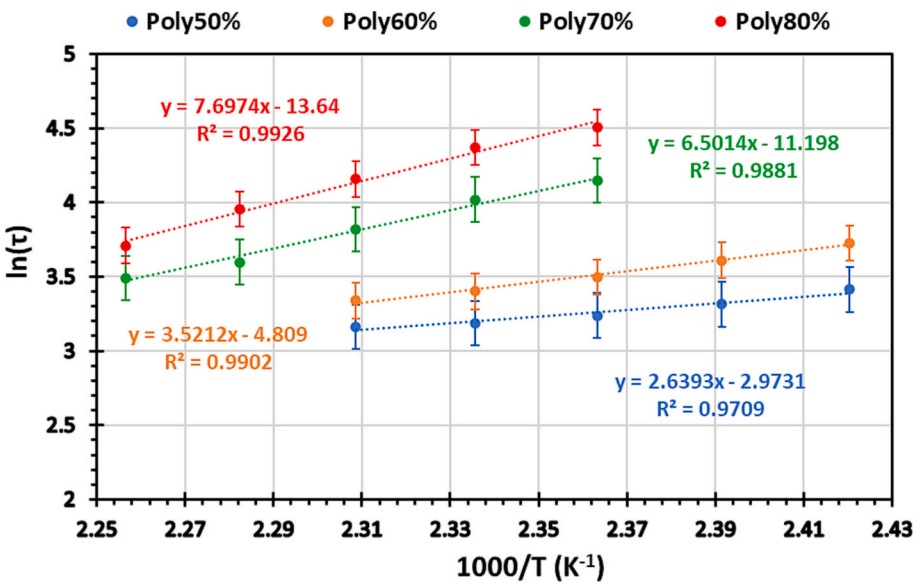

Fig. 6. Arrhenius plot of relaxation times against the inverse of the temperature for the different materials prepared.

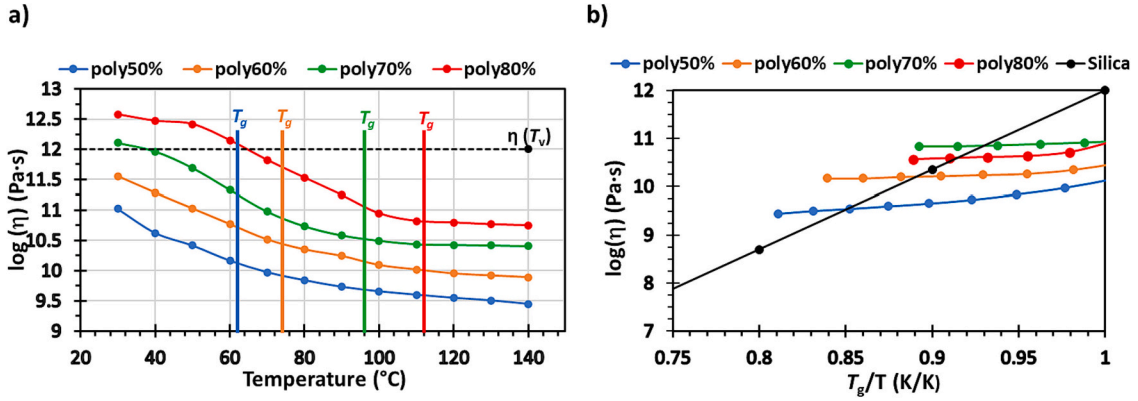

Fig. 7. a) Evolution of the viscosity with temperature for all the materials prepared and b) Angell fragility plot of all materials including vitreous silica as a reference of an ideal strong liquid.

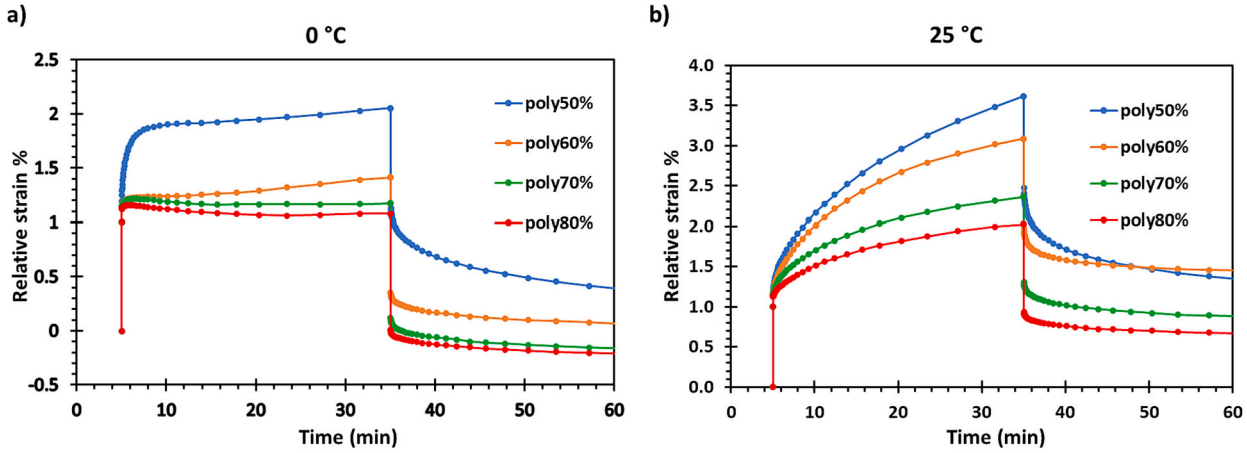

Fig. 8. Creep and recovery curves of all the materials at 0 °C (a) and 25 °C (b).

of all the materials (see Fig. S8). In any case, no evidence of dynamic processes can be seen in the creep tests at 0 °C. On the contrary, at 25 °C, all materials present a more evident creep behavior when the stress is applied, and in the recovery process, a permanent deformation remains due to the topological effect of the chains. It is essential to point out a clear increase in the creep resistance when the content of the aromatic epoxy resin is higher. Indeed, poly80%, which is the material that contains the highest proportion of TGAP, only presents a slight plastic deformation, even maintaining extremely fast relaxation rates at 140 °C, highlighting the great potential of this type of materials.

3.4. Study of the self-healing and self-welding abilities

Vitrimeric materials present significant advantages in their applicability compared to conventional thermosets. Two of the most important applications in this field are self-healing and self-welding abilities, among many others [31,32]. In order to evaluate these properties, poly80% was selected because it has the higher T_g, lower plastic deformation, and slowest relaxation rates. Therefore, it is the material with a predictable lower self-healing ability. To study this property, controlled indentations with a spherical indenter and with different pressures ranging from 306 MPa to 360 MPa were applied on the sample. After performing the indentations, the sample was left for 24 h at room temperature to ensure no viscoelastic recovery. Subsequently, it was heated up to 160 °C, controlling the recovery process at different times. The evolution of the dimension of the indentations made on the surface of the poly80% is shown in Fig. 9.

As can be seen, no viscoelastic recovery was produced at room temperature for 24 h. However, when the sample was heated up to 160 °C, the material completely self-healed all the indentations at different pressures in only 2 min. This highlights the outstanding capability to undergo self-healing and, therefore, the great potential in the industrial field.

To study the self-welding, a dog-bone sample of poly80% was broken into two pieces under liquid nitrogen, put in a mold to ensure the maximum contact between the two breaking surfaces, and heated at 160 °C for 2 h. As can be seen in Fig. 10, the two parts were perfectly attached after the procedure. To quantitively test this ability, the virgin and the welded samples were subjected to a tensile test to obtain their mechanical strength (Fig. S9). As shown in Table 4, both samples presented the same Young Modulus (E), which means similar mechanical behavior. Despite this, the strength of the welded sample was considerably lower than the virgin one, clearly due to an imperfect contact between the two broken parts during the heating process. The welded surface may present micro-voids due to the absence of small parts of material that start the failure process.

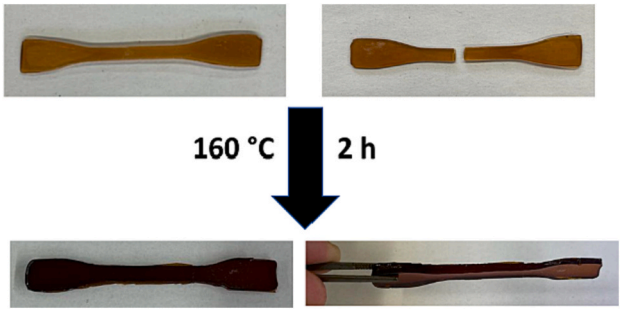

Fig. 10. Pictures taken to the original sample, the broken one under nitrogen and the self-welded.

Table 4
Stress and strain at break and Young Modulus of the virgin and welded samples.

Sample	σ_b (MPa)	ε_b (%)	E (MPa)
Virgin	73	4.2	2726
Welded	24	1.0	2630

4. Conclusions

A series of disulfide vitrimeric materials were successfully prepared using a straightforward epoxy-amine condensation reaction between two commercially available epoxy resins, one aromatic resin (TGAP), and one aliphatic resin (HDGE) along with cystamine serving as the amine crosslinker containing the disulfide bonds. By varying the proportions of the epoxy resins, we achieved precise control over the thermomechanical and viscoelastic properties of the final materials.

The completion of the curing reaction was effectively confirmed through FTIR analysis by the disappearance of the epoxy bands. The prepared materials exhibited excellent thermal stability up to 200 °C, enabling safe stress-relaxation tests below this temperature. DMA analysis further revealed high T_gs (above 60 °C) for all materials, with

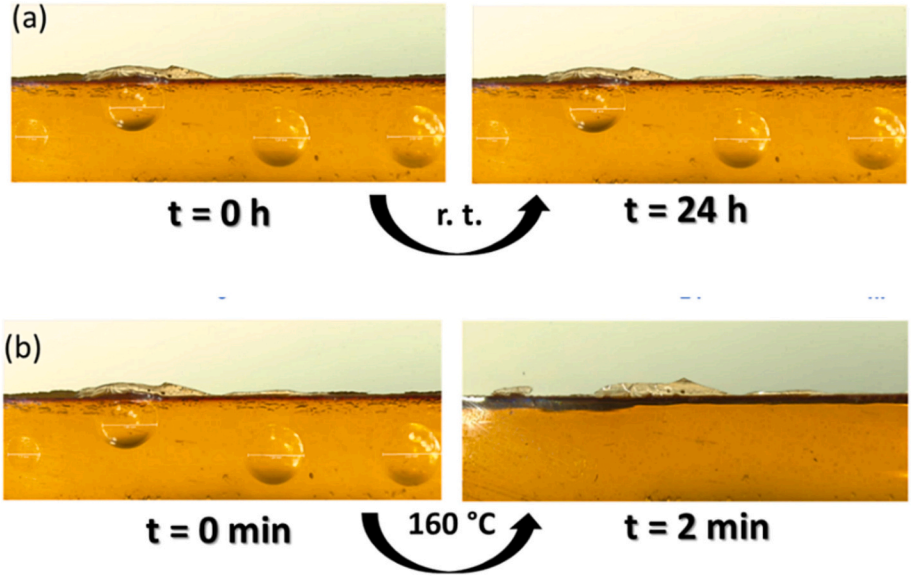

Fig. 9. Evolution of the indentations at room temperature (a) and at 160 °C (b) made on poly80%.

enhanced rigidity in the glassy state, particularly when the proportion of TGAP was increased.

The viscoelastic properties and the vitrimeric behavior were studied via stress-relaxation tests which revealed that all materials could relax the initial stress in less than 1 min at 160 °C. To characterize the materials' creep response, we conducted creep experiments, resulting in topology freezing temperatures (Tv) below the glass transition temperature, with a clear upward trend observed as the aromatic epoxy resin content in the samples increased. Furthermore, creep tests performed at 0 °C and 25 °C demonstrated that samples with higher TGAP content exhibited superior creep resistance at service temperatures. Finally, to test the mechanical behavior and their functional properties, tensile tests, self-healing, and self-welding tests were conducted. The results showcased high values of stress and strain at break for the virgin sample, rapid self-healing capabilities (within 2 min at 160 °C), and promising welding ability. These observations underscore the technological potential of these materials, driven by their easy preparation, excellent thermomechanical properties, and versatile applicability across a wide range of applications.

Author contributions

A.R. and *V*.D. prepared the materials and performed the experimental tests. A.R. wrote the original draft. S. D. F. and A. S. validated the studies, made conceptualization, supervised the work, and reviewed and edited the final manuscript.

Declaration of Competing Interest

The authors declare that they have no known competing financial interests or personal relationships that could have appeared to influence the work reported in this paper.

Data availability

Data will be made available on request.

Acknowledgments

This work is part of the R&D project PID2020-115102RB-C21 and TED2021-131102B-C22 funded by MCNI/AEI/10.13039/501100011033 and European Union NextGeneration EU/PRTR. We also want to thank Generalitat de Catalunya (2021-SGR-00154).

Appendix A. Supplementary data

Supporting Information. Structural characterization of cystamine, creep, thermomechanical analysis (loss moduli) and dilatometry and tensile tests. Supplementary data to this article can be found online at [https://doi.org/10.1016/j.reactfunctpolym.2023.105764].

References

[1] G.M. Scheutz, J.J. Lessard, M.B. Sims, B.S. Sumerlin, Adaptable crosslinks in polymeric materials: resolving the intersection of thermoplastics and thermosets, J. Am. Chem. Soc. 141 (2019) 16181–16196, https://doi.org/10.1021/jacs.9b07922.

[2] M. Podgórski, B.D. Fairbanks, B.E. Kirkpatrick, M. McBride, A. Martinez, A. Dobson, N.J. Bongiardina, C.N. Bowman, Toward stimuli-responsive dynamic thermosets through continuous development and improvements in covalent adaptable networks (CANs), Adv. Mater. 32 (2020) 1906876, https://doi.org/10.1002/adma.201906876.

[3] D. Montarnal, M. Capelot, F. Tournilhac, L. Leibler, Silica-like malleable materials from permanent organic networks, Science 334 (2011) 965–968, https://doi.org/10.1126/science.1212648.

[4] T. Liu, C. Hao, L. Wang, Y. Li, W. Liu, J. Xin, J. Zhang, Eugenol-derived biobased epoxy: shape memory, repairing and recyclability, Macromolecules 50 (2017) 8588–8597, https://doi.org/10.1021/acs.macromol.7b01889.

[5] D. Berne, F. Cuminet, S. Lemouzy, C. Joly-Duhamel, R. Poli, S. Caillol, E. Leclerc, V. Ladmiral, Catalyst-free epoxy vitrimers based on transesterification internally activated by an α-CF_3 group, Macromolecules 55 (2022) 1669–1679, https://doi.org/10.1021/acs.macromol.1c02538.

[6] A. Roig, A. Petrauskaitė, X. Ramis, S. De la Flor, À. Serra, Synthesis and characterization of new bio-based poly(acylhydrazone) vanillin vitrimers, Polym. Chem. 13 (2022) 1906876, https://doi.org/10.1039/d1py01694f.

[7] A. Roig, P. Hidalgo, X. Ramis, S. De la Flor, À. Serra, Vitrimeric epoxy-amine polyimine networks based on a renewable vanillin derivative, ACS Appl. Polym. Mater. 4 (2022) 9341–9350, https://doi.org/10.1021/acsapm.2c01604.

[8] W. Denissen, M. Droesbeke, R. Nicolaÿ, L. Leibler, J.M. Winne, F.E. Du Prez, Chemical control of the viscoelastic properties of vinylogous urethane vitrimers, Nat. Commun. 8 (2017) 14857, https://doi.org/10.1038/ncomms14857.

[9] S. Engelen, A.A. Wróblewska, K. De Bruycker, R. Aksakal, V. Ladmiral, S. Caillol, F. E. Du Prez, Sustainable design of vanillin-based vitrimers using vinylogous urethane chemistry, Polym. Chem. 13 (2022) 2665–2673, https://doi.org/10.1039/D2PY00351A.

[10] C. Chapelle, B. Quienne, C. Bonneaud, G. David, S. Caillol, Diels-Alder-chitosan based dissociative covalent adaptable networks, Carbohydr. Polym. 253 (2021), 117222, https://doi.org/10.1016/j.carbpol.2020.117222.

[11] X. Xu, S. Ma, S. Wang, B. Wang, H. Feng, P. Li, Y. Liu, Z. Yu, J. Zhu, Fast-reprocessing, postadjustable, self-healing covalent adaptable networks with Schiff Base and Diels-Alder adduct, Macromol. Rapid Commun. 43 (2022) 2100777, https://doi.org/10.1002/marc.20210077.

[12] B.R. Elling, W.R. Dichtel, Reprocessable cross-linked polymer networks: are associative exchange mechanisms desirable? ACS Cent. Sci. 6 (2020) 1488–1496, https://doi.org/10.1021/acscentsci.0c00567.

[13] F. Gamardella, S. Muñoz, S. De la Flor, X. Ramis, A. Serra, Recyclable organocatalyzed poly(thiourethane) covalent adaptable networks, Polymers 12 (2020) 2913, https://doi.org/10.3390/polym12122913.

[14] F. Guerrero, X. Ramis, S. De la Flor, À. Serra, Preparation and characterization of a series of self-healable bio-based poly(thiourethane) vitrimer-like materials, Polymers 15 (2023) 1583, https://doi.org/10.3390/polym15061583.

[15] Y. Oba, T. Kimura, M. Hayashi, K. Yamamoto, Correlation between self-assembled nanostructures and bond exchange properties for polyacrylate-based vitrimer-like materials with a trans-*N*-alkylation bond exchange mechanism, Macromolecules 55 (2022) 1771–1782, https://doi.org/10.1021/acs.macromol.1c02406.

[16] Q. Li, S. Ma, N. Lu, J. Qiu, J. Ye, Y. Liu, S. Wang, Y. Han, B. Wang, X. Xu, H. Feng, J. Zhu, Concurrent thiol-ene competitive reactions provide reprocessable, degradable and creep-resistant dynamic-permanent hybrid covalent adaptable networks, Green Chem. 22 (2020) 7769–7777, https://doi.org/10.1039/D0GC02823A.

[17] A. Ruiz de Luzuriaga, G. Solera, I. Azcarate-Ascasua, V. Boucher, H.-J. Grande, A. Rekondo, Chemical control of the aromatic disulfide exchange kinetics for tailor-made epoxy vitrimers, Polymers 239 (2022), 124457, https://doi.org/10.1016/j.polymer.2021.124457.

[18] K. Yamawake, M. Hayashi, The role of tertiary amines as internal catalysts for disulfide exchange in covalent adaptable networks, Polym. Chem. 14 (2023) 680, https://doi.org/10.1039/d2py01406h.

[19] L. Li, X. Chen, J.M. Torkelson, Covalent adaptive networks for enhanced adhesion: exploiting disulfide dynamic chemistry and annealing during application, ACS Appl. Polym. Mater. 2 (2020) 4658–4665, https://doi.org/10.1021/acsapm.0c00720.

[20] S. Guggari, F. Magliozzi, S. Malburet, A. Graillot, M. Destarac, M. Guerre, Vanillin-based epoxy vitrimers: looking at the cystamine hardener from a different perspective, ACS Sustain. Chem. Eng. 11 (2023) 6021–6031, https://doi.org/10.1021/acsuschemeng.3c00379.

[21] A. Roig, M. Agizza, À. Serra, S. De la Flor, Disulfide vitrimeric materials base don cystamine and diepoxy eugenol as bio-based monomers, Eur. Polym. J. 19 (2023), 112185, https://doi.org/10.1016/j.eurpolymj.2023.112185.

[22] F. Van Lijsebetten, T. Debsharma, J.M. Winne, F.E. Du Prez, A highly dynamic covalent polymer network without creep: mission impossible? Angew. Chem. Int. Ed. 61 (2022), e202210405 https://doi.org/10.1002/anie.202210405.

[23] L. Li, X. Chen, K. Jin, J. Torkelson, Vitrimers designed both to strongly suppress creep and to recover original cross-link density after reprocessing: quantitative theory and experiments, Macromolecules 51 (2018) 5537–5546, https://doi.org/10.1021/acs.macromol.8b00922.

[24] F. Van Lijsebetten, K. De Bruycker, Y. Spiesschaert, J.M. Winne, F.E. Du Prez, Suppressing creep and promoting fast reprocessing of vitrimers with reversible trapped amines, Angew. Chem. Int. Ed. 61 (2022), e202113872, https://doi.org/10.1002/anie.202113872.

[25] W. Denissen, J.M. Winne, F.E. Du Prez, Vitrimers: permanent organic networks with glass-like fluidity, Chem. Sci. 7 (2016) 30–38, https://doi.org/10.1039/C5SC02223A.

[26] K.F. Kelton, Kinetic and structural fragility-a correlation between structures and dynamics in metallic liquids and glasses, J. Phys. Condens. Matter 29 (2017), 023002, https://doi.org/10.1088/0953-8984/29/2/023002.
[27] C.A. Angell, Formation of glasses from liquids and biopolymers, Science 267 (1995) 1924–1935, https://doi.org/10.1126/science.267.5206.1924.
[28] A.M. Hubbard, Y. Ren, C.R. Picu, A. Sarvestani, D. Konkolewicz, A.K. Roy, V. Varshney, D. Nepal, Creep mechanics of epoxy vitrimer materials, ACS Appl. Polym. Mater. 4 (2022) 4254–4263, https://doi.org/10.1021/acsapm.2c00230.
[29] A.M. Hubbard, Y. Ren, D. Konkolewicz, A. Sarvestani, C.R. Picu, G.S. Kedziora, A. Roy, V. Varshney, D. Nepal, Vitrimer transition temperature identification: coupling various thermomechanical methodologies, ACS Appl. Polym. Mater. 3 (2021) 1756–1766, https://doi.org/10.1021/acsapm.0c01290.
[30] X. Shi, Q. Ge, H. Lu, K. Yu, The nonequilibrium behaviors of covalent adaptable network polymers during the topology transition, Soft Matter 17 (2021) 2104, https://doi.org/10.1039/d0sm01471k.
[31] A. Khan, N. Ahmed, M. Rabnawaz, Covalent adaptable network and self-healing materials: current trends and future prospects in sustainability, Polymers 12 (2020) 2027, https://doi.org/10.3390/polym12092027.
[32] A. Vashchuk, Y. Kobzar, Chemical welding of polymer networks, Mater. Today Chem. 24 (2022), 100803, https://doi.org/10.1016/j.mtchem.2022.100803.